Norwegian Meteorological Institute
met.no
met.no report
no. 10/2006
Remote sensing

Use of ASAR wave spectra in operational wave analysis and forecasting

Report from the EnviWave project

Hanne Heiberg
Lars-Anders Breivik
Magnar Reistad
Alvin Brattli

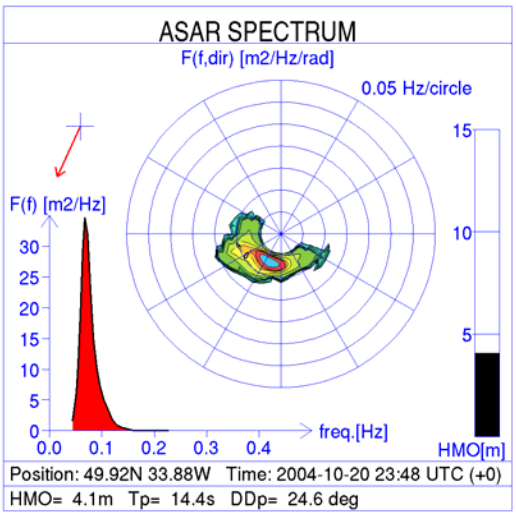

Polar plot of ASAR derived wave spectrum

Norwegian Meteorological Institute met.no

report

Title Use of ASAR wave spectra in operational wave analysis and forecasting	**Date** 14 December 2006
Section Remote sensing	**Report no.** 10
Author(s) Hanne Heiberg, Lars-Anders Breivik, Magnar Reistad, Alvin Brattli (current affiliation: Norwegian Defence Research Establishment (FFI))	**Classification** ☐ Free ☒ Restricted
	ISSN 1503-8025
	e-ISSN 1503-8025
Client(s) EU	**Client's reference** EVG1-CT-2001-00051

Abstract

The ENVISAT satellite is serving the user community with geophysical ocean wave products. This study focuses on optimal use of ASAR data provided by the ENVISAT satellite in operational wave monitoring and forecasting. To exploit the ASAR data in terms of improved wave spectra, an assimilation technique was developed based on the state of the art analysis and model systems. A method for optimal analysis and assimilation of 2-dimensional wave spectra has been implemented in the HIRLAM-WAM system at the Norwegian Meteorological Institute, met.no. The quality of the wave spectra assimilation has been validated in an impact study with ENVISAT data from the winter season in the Norwegian sea and the North Atlantic ocean.

Keywords

Wave spectra, wave heights, SAR, ASAR, model, assimilation, nowcasting, forecasting, modeling, remote sensing, wave propagation, wave analysis

Disiplinary signature	Responsible signature
_____	_____

Postal address P.O.Box 43, Blindern NO-0313 OSLO Norway
Office Niels Henrik Abelsvei 40
Telephone +47 22 96 30 00
Telefax +47 22 96 30 50
e-mail: met@met.no **Internet:** met.no
Bank account 7694 05 00628
Swift code DNBANOKK

Postal address
P.O.Box 43, Blindern
NO-0313 OSLO
Norway

Office
Niels Henrik Abelsvei 40

Telephone
+47 22 96 30 00

Telefax
+47 22 96 30 50

e-mail: met@met.no
Internet: met.no

Bank account
7694 05 00628

Swift code
DNBANOKK

1. Background

The ASAR spectra give good information on long wave part (swell) of the ocean waves. For oil rigs and vessels accurate nowcasting and short term forecasting of long waves is of great importance. Such installations are sometimes exposed to large vertical movements, i.e. heave. Each rig responds differently to waves, but it is common that large rigs have a resonance period around 20 s. Such long waves may give vertical movements in the rig twice as large as the wave height. If this kind of vertical movement comes unexpectedly drilling has to be interrupted suddenly. This is expensive and there is also a risk of blow out and serious oil pollution.

Improved swell nowcasting and forecasting in ocean areas are also important for forecasting of swell in coastal areas and harbors. Long period swell with only modest height is known to cause serious problems in some harbors when the wave direction and wave period are unfavorable. Improved information on the spectral distribution of the energy of long waves at the inlets to fjords and harbor areas will increase the possibility to make detailed swell forecasts in these areas by use of local wave models.

SAR derived wave spectra has been used at the Norwegian Meteorological Institute, met.no, in connection with utilization of data from the ERS-1 and -2 satellites [*Breivik et al.*, 1998]. The wave spectra derived from the SAR onboard the ERS satellites were received in near real time. Both wave spectra derived from data received via the meteorological network GTS as ami wave mode, and wave spectra derived from image mode data received at Tromsø Satellite Station were used. The data were found to contain valuable information in the long wave swell part of the wave spectra. However the SAR derived wave spectra proved to be rather dependent on first guess wave spectra normally taken from an operational wave model. In the short wave, wind sea part of the spectra, there was no independent information from SAR.

A method to assimilate the ERS SAR derived wave spectra in the operational wave model at met.no was developed, implemented and tested in a five-month winter test period [*Breivik et al.*, 1998]. The impact compared to an operational model running without SAR data, were found to be small but slightly positive. Two main reasons for limitation of impact were found to be:

1. Low data coverage. There were normally 400 km between each SAR derived wave spectra.
2. Dependency of the SAR derived wave spectra on the wave model first guess.

When ENVISAT ASAR data finally arrived in 2002 these two issues were supposed to be significantly improved. The introduction of ASAR wave mode data should ensure stable supply of observed wave spectra over open seas. As will be shown in this report, this has proven to be difficult for the areas of interest in this study.

Further, a new inversion algorithm was developed for ASAR data and implemented operationally [*Engen et al.*, 2000]. In contrast to the method used to derive wave spectra from ERS data in 1998, this algorithm is independent of first guess data and has proven to give reasonable quality wave spectra information in the swell part of the spectra. In the current study a new method to assimilate the full ASAR derived wave spectra in the wave model WAM on a limited area has been developed, implemented and tested.

Several studies have been reported with assimilation of characteristic mean parameters of SAR derived wave spectra [*Hasselmann et al.*, 1997; *Aouf et al.*, 2006; *Bidlot*, 2002], and directional buoy spectra [*Voorrips et al.*, 1997], in contrary to the full 2-dimensional wave spectra. They apply spectral wave partitioning schemes where spectral information is decomposed into one or more wave partitions or wave systems. For each wave system a set of characteristic mean parameters is determined, e.g. wave energy component, mean direction, and mean frequency [*Hasselmann et al.*, 1997; *Voorrips et al.*, 1997; *Bidlot*, 2002]. The wave partitions in the model spectra are adjusted and cross assigned to corresponding wave partitions of the SAR spectra. Then the limited number of characteristic mean parameters is used in the

assimilation. The analyzed spectra are reconstructed by rescaling and reshaping the model spectra, based on the mean parameters obtained from the assimilation.

The spectral partitioning schemes are used mainly for two reasons: the low computational cost and the avoiding of discontinuities due to the cut-off wavelengths of SAR/ASAR. Cross assignment of wave partitions is safe when the partitions match relatively closely. However, that is not always the case and wrong assignments may occur. In some cases wave systems may simply be unmatched, and it is not obvious how to handle this optimally, particularly not unmatched wave systems in observed spectra. *Voorrips et al.* [1997] have chosen to cross assign an initially unmatched observed wave system to a model wave system within 90 degrees of rotation, or otherwise discard the observation. *Hasselmann et al.* [1997] have chosen to superimpose unmatched wave systems on the first-guess spectra. Either way, the assimilation of only a few mean parameters, implies that a significant part of the information in the observed wave spectra may get lost. Such algorithms may be more robust with respect to poor observation quality, but will not have the same potential of improving the results in a geographically limited model area, since it may basically filter out swell that has been generated entirely outside the model area and therefore is not present in the model state.

A global model describes swell significantly better than a local model, and observations of swell not present in the global model state is less likely and hence probably less reliable. The limited WAM model area used at met.no (see Figure 1) does not cover the entire swell generating region, and it is impossible for the model to include the swell originating outside the model area properly. Observations of swell that is not present in the model state are likely. These observations are potentially of extra large value in improving the forecast. Based on these considerations, as well as our previous experience with assimilation of the full SAR derived wave spectra [*Breivik et al.*, 1998], we have chosen to further develop the assimilation scheme of 2-dimensional wave spectra.

In the current study the model and observation wave spectra are uncorrelated, since the ENVISAT ASAR derived wave spectra are retrieved completely independent of the model. We aim to reduce the discontinuity problem by using an observation error covariance matrix (**R**), which smoothly reduces the weight/impact of the ASAR observation for frequencies approaching the cut-off frequency. The **R**-matrix also correlates neighboring frequency and directional bins. In addition, the observation operator contains a low-pass filter that increasingly reduces the model energies for increasing frequencies. This will be described in further detail below.

The assimilation scheme is implemented for the wave model WAM. WAM is the main tool for operational wave forecasting at met.no, and it plays an important role in all parts of this report. The WAM model run at met.no is a regional adapted version of the WAM Cycle 4 model. This is a third generation wave model developed by the international WAMDI group [1988]. At met.no it runs operationally with 50 km horizontal resolution covering North Atlantic and the sea areas around Norway (Figure 1). Wind input to the WAM model is output from the operational limited area numerical weather prediction model HIRLAM.

The methods and results are described in the following chapters. The presented work is results from an EU Fifth Framework project, EnviWave, where aim was to investigate the quality and potential use of ocean wave data obtained from the ENVISAT platform [*Johnsen*, 2005a].

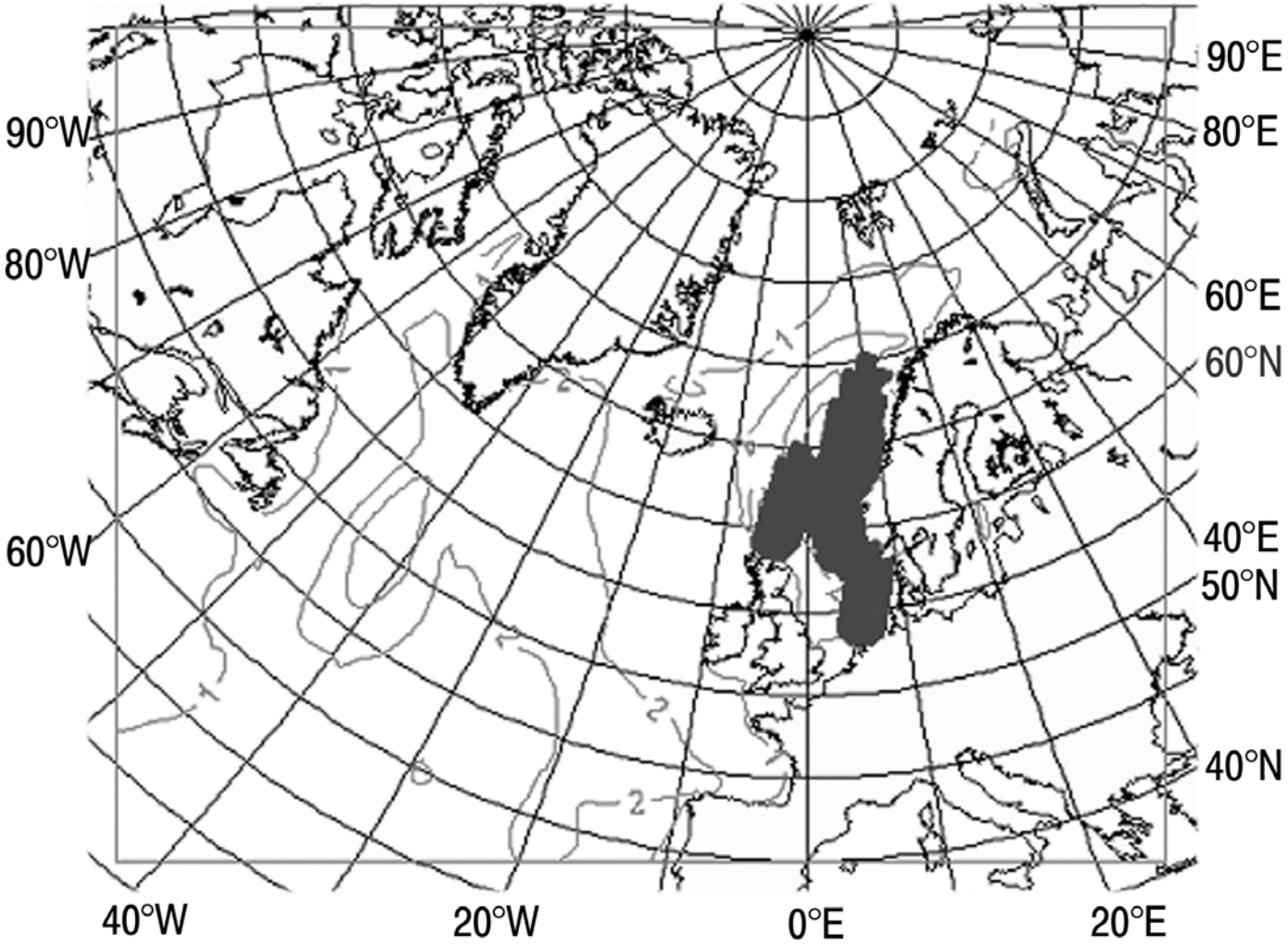

Figure 1: WAM model grid applied in the present work. Black solid area shows locations of ASAR Image Mode data from the North Sea and the Norwegian Sea, Jan. 2005, data set 3.

2. Assimilation of ASAR data in the wave model at met.no

A method for assimilation of SAR derived wave spectra was developed at met.no for use of ERS-1 and -2 data [*Breivik et. al.*, 1998]. Different from other attempts on wave spectra assimilation, e.g. *Hasselmann et al.* [1997], the idea was to assimilate the full wave spectra. A challenging problem then is how to describe the error covariance between the frequency and direction bins in the spectra. In 1998 this was solved pragmatically by treating each bin separately, which is equivalent to ignore error correlations between bins. The analysis equations were then solved using a version of statistical interpolation.

In the EnviWave project a new analysis and assimilation scheme has been developed which allows for a more realistic treatment of error covariances. Method and results are described below.

2.1. Description of the ASAR assimilation algorithm

The ASAR assimilation algorithm follows the PSAS scheme, which is a dual formulation [*Bouttier and Courtier*, 2002] of optimal interpolation (OI) and 3DVAR. The classical OI scheme is given by:

$\mathbf{x_a} = \mathbf{x_b} + \mathbf{B}\mathbf{H}^T (\mathbf{R} + \mathbf{H}\mathbf{B}\mathbf{H}^T)^{-1} (\mathbf{y} - \mathrm{H}\,\mathbf{x_b})$ (1)

where **y** is obs. state, $\mathbf{x_b}$ is first-guess (background) state, and $\mathbf{x_a}$ is the analyzed state, all represented as vectors. **B** and **R** are error covariance matrices for background and observations, respectively. H is the observation operator and **H** is the linearized observation operator.
In the PSAS scheme equation (1) is rewritten to

$\mathbf{w_a} = (\mathbf{R} + \mathbf{H}\mathbf{B}\mathbf{H}^T)^{-1} (\mathbf{y} - \mathrm{H}\,\mathbf{x_b})$ (2)
$\mathbf{x_a} = \mathbf{x_b} + \mathbf{B}\mathbf{H}^T\ \mathbf{w_a}$ (3)

In the present implementation eq. (2) is solved for $\mathbf{w_a}$ iteratively, using the preconditioned conjugated gradient method (CGM) with domain decompositioning as preconditioner [*Aarnes*, 2003]. The preconditioner is used to solve subproblems of the matrix equations and speed up the calculation.

The observation operator **H**, linearly interpolates the background spectrum from the background spectral domain to the observation domain. **H** also contains a low-pass filter, which reduces the energies of the WAM spectrum increasingly for increasing frequencies, by multiplying the energy of each frequency bin no. *i* (for all *i*), with a factor:

$K_{low\_pass\_filter}(i) = 1.0/\ \mathrm{sqrt}(1+(f_i / 0.061159\ \mathrm{Hz})^4)$

f_i is the ASAR frequency number *i* in Hz. 0.061159 Hz is the frequency of frequency number 5 in WAM. ASAR energies for high frequencies are generally zero because the ASAR instrument is not able to detect waves of high frequencies, in contrast to the wave model. The low-pass filter acts by downscaling this (unphysical) difference, as part of the observation operator.

In the applied assimilation scheme each observation is moved to its closest grid point in the model grid. The background error covariance matrix let the assimilated spectrum affect the model spectra of all grid points within the influence radius. The scheme does not take into account wave reducing effects from islands between the "observation grid point" and the influence radius.

The problem of data assimilation will not be discussed further here, and the reader is referred to textbooks on the topic [*Kalnay*, 2003]. For further and more technical information about the computer code of assimilation, see the document by *Heiberg and Brattli* [2005].

2.2. Error covariances

The assimilation scheme implemented in the present work, Physical Space Assimilation System (PSAS), involves the background error covariance matrix (**B**) and the observation covariance matrix (**R**):

$\mathbf{w_a} = (\mathbf{R} + \mathbf{H}\mathbf{B}\mathbf{H}^T)^{-1} (\mathbf{y} - \mathrm{H}\,\mathbf{x_b})$
$\mathbf{x_a} = \mathbf{x_b} + \mathbf{B}\mathbf{H}^T\,\mathbf{w_a}$

The relative weight between **B** and **R** controls how much we let the observation spectrum, **y**, affect the analyzed (assimilated) spectrum, $\mathbf{x_a}$.

2.3. Background error covariance matrix, B

The background covariance matrix, **B**, enforces assimilation influence between geographical locations within the influence radius (400 km), as well as in the spectral domain, between neighboring frequencies and directions. In this way **B** spreads and smoothes the information in the analyzed spectrum, $\mathbf{x_a}$. The **B** matrix is block diagonal with the chosen values

- 1.0 on the diagonal

- 0.1 for neighboring frequencies and neighboring directions
- 0.01 for bins that are neighbors both with respect to frequencies and directions

2.4. Observation covariance matrix, R

The observations are assumed to be uncorrelated in both space and spectral domain, and the observation covariance matrix, **R**, is diagonal. We have chosen to let the diagonal values of **R** be specific for each frequency and equal for all directions.

The **R** element values are normally found by statistical studies on the observations vs. the best independent reference available. In the ideal situation the observation correlation should be estimated independently from the model, but this is unfortunately not possible for the ASAR derived wave spectra. In stead we estimate the error relative to the WAM model. The result of the statistical study in the present work is described in the next section. The statistical study shows a somewhat weak relation between bins of the ASAR derived wave spectra vs. the corresponding bins of the reference WAM model wave spectra. The results are therefore not enough to properly determine the **R** matrix and a set of qualitative tests have also been performed, as described in the section "Qualitative tests of R matrices" below.

It is important to point out that comparison between model and observed spectra at bin level, is a comparison of waves at very high resolution. At such high resolution there is not necessarily a very strong correlation in every bin, even though the observed wave spectra contain valuable and reliable information and the assimilation scheme works efficiently for the present purpose.

3. Statistical study of ASAR derived wave spectra

The 2-dimensional ASAR derived wave spectrum consists of 24 frequencies ([0.044157,..., 0.228080] Hz) in 36 directions, i.e. 24*36 bins of observation values. The complete list of ASAR frequencies is given in Table 2. We will refer to a general bin in the spectrum as {freq(i), dir(j)}. The WAM model spectrum consists of 25 frequencies ([0.041772,..., 0.411450] Hz) in 24 directions.

The quality and error estimate of observations should ideally be based on comparison with very accurate data coinciding in time and space. However, due to lack of reliable data coinciding with ASAR observations, the quality and error estimates of ASAR wave spectra are based on comparison with WAM model spectra. The statistics in each bin {freq(i), dir(j)} are therefore based on the difference between ASAR wave energies and collocated WAM model energies interpolated to the ASAR domain.

3 data sets of ASAR wave spectra have been studied.
Data set

1. ASAR Wave Mode data from the winter season Nov. 2003 – Mar. 2004,
2. ASAR Wave Mode data of 1 month from Jan. 2004 (subset of data set 1.),
3. ASAR Image Mode data of 1 month from Jan. 2005.

3.1. Data set 1: winter season Nov. 2003 – Mar. 2004

Data set 1 (and 2) show large variations between ASAR and WAM. In about 40 % of all the bins (i.e. {freq(i), dir(j)}) the mean difference between ASAR and WAM energies are larger than either the mean ASAR energy or mean WAM energy. The result indicates a systematic deviation between ASAR and WAM in a large part of the spectra. In general one should be very cautious when assimilating observations that show large systematic deviations from the wave model.

3.2. Data set 2: 1 month's subset of ASAR Wave Mode data

In order to extract more information from the data, statistics were performed on a subset of the data with 2800 spectra from January 2004. This subset is referred to as data set 2. Scatter plots with ASAR energy vs. WAM energy for each bin {freq(i), dir(j)}, were analyzed with linear regression. For most bins the scatter plots had clouds along the axes, or in no particular direction, and the energies were approximately zero.

A diagnostic parameter R^2 was calculated for every bin

$R^2 = 1 - \text{Sum}(R(i)^2) / \text{Sum}((y(i) - y')^2)$, $0 < R < 1$.

y' is the mean of y(i) if there is an intercept and zero otherwise. R^2 gives the fraction of variance explained by the linear regression model, see left panel in Figure 2. This indicates how well the variation in the data is explained by linear regression ($0 < R^2 < 1$). It is not recommended to trust ASAR for wave lengths below 250 m (0.079 Hz), i.e. above frequency no. 9 [*Kerbaol et al.*, 1998; *Hasselmann and Hasselmann*, 1991]. Figure 2 supports this. However, the R^2 values are also much lower than we expected for frequency no. 1-9, indicating that the relation between corresponding bins of ASAR observations and WAM model is generally not very strong and that the data set is rather inadequate for implementation of the observation error covariance matrix. We therefore decided to repeat our study on a new, carefully checked data set, with focus on the North Sea and Norwegian Sea.

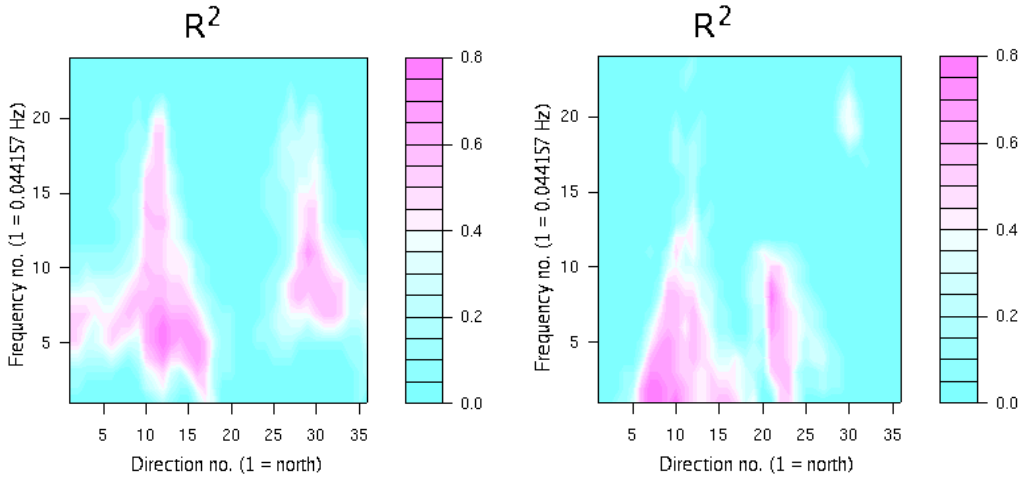

Figure 2: Diagnostic parameter R^2 is calculated for each bin ({freq(i), dir(j)}) with respect to 24 different frequencies along the vertical axis and the 36 directions along the horizontal axis. See Table 2 for the frequency numbers in Hz and m^{-1}. **Left**: Wave spectra derived from ASAR *Wave Mode* data, Jan. 2004, data set 2. **Right:** Wave spectra derived from ASAR *Image Mode*, Jan. 2005, data set 3.

3.3. Data set 3: ASAR Image Mode data

ASAR Wave Mode data in the North Sea and Norwegian Sea are very scarce and therefore a set of ASAR Image Mode data was ordered for this region for January 2005 (see Figure 1). A data set of 915 wave spectra from 7 days was obtained from Kongsberg Satellite Station (KSAT), and carefully quality checked by NORUT. This is referred to as data set 3. The quality of this set was expected to be at least as good as the previous data set from January 2004, and as good as we could possibly get from ASAR Wave Mode on operational basis. The same statistical study as for data set 2 was repeated. The right panel in Figure 2 shows the diagnostic R^2 parameter values for each bin {freq(i), dir(j)}. This data set also shows a lot of low R^2 values indicating a rather weak relation between corresponding bins in ASAR wave spectra and the collocated model spectra.

3.4. General discussion of statistical study

It is worth to note that there are other reasons for low R^2 values than lack of correlation. For many bins R^2 is zero because the ASAR energies are zero, while the model energies are only close to zero. This is

exemplified in this study, too. Most of our data are located close to the coast. There is very little swell sea heading off the coast, and ASAR is expected to show little energy in these directions. The mean ASAR energy is indeed zero for many bins in directions off the coast, while the WAM energies are only close to zero. This gives $R^2 = 0$ (see Figure 2), although it is not really due to lack of correlation.

ASAR and WAM usually give maximum energy in the same frequency and direction. However, for the low frequent part of the swell (0.05-0.07 Hz), ASAR tend to show waves in a significantly wider range of directions than WAM, see Figure 3, 5, 9, and 11. For ASAR these low frequent waves often have a range of 210 deg., while (non-assimilated) WAM usually gives waves within a significantly smaller range, more in the order of 150 deg. There are also observations where ASAR shows swell heading right off the coast like in Figure 3. We suspect that the range of directions in ASAR spectra is unrealistically large. It is known that the quality of ASAR wave spectra is somewhat reduced in azimuth direction [*Johnsen*, 2005b; *Fouques et al.*, 2005], and it is likely that this contributes to the large range of directions of the ASAR "wings".

The dominant wind and swell directions from west in the area of the present data sets are not an optimal basis for estimating error covariances with respect to directions. Based on these considerations, it was decided to set the covariance values for each frequency equal for all directions.

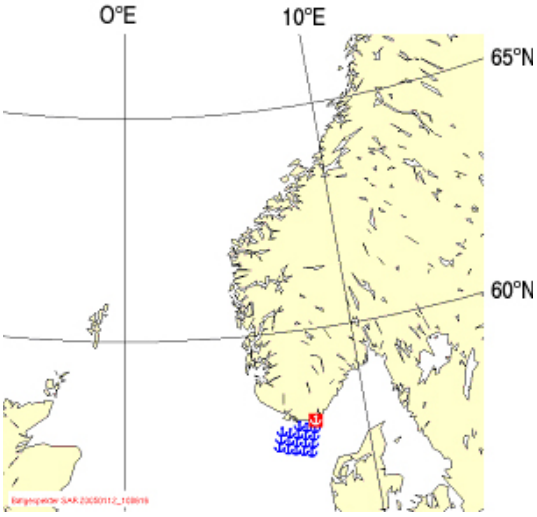

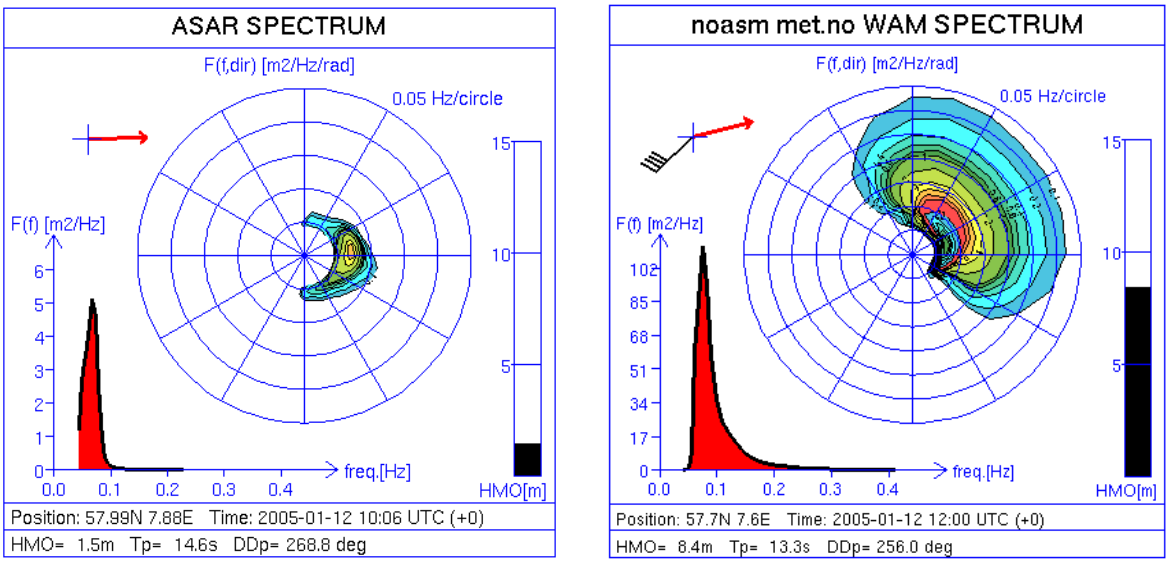

Figure 3: Location of ASAR spectrum (red and white anchor in top panel), ASAR spectrum with part of swell going southwards right off the coast (bottom left panel), non-assimilated WAM spectrum in the nearest WAM grid point (bottom right panel).

3.5. Comparison of characteristic mean parameters

The ASAR Image Mode data in data set 3 have also been compared with collocated WAM data with respect to significant wave height, peak period and mean period, see Figure 4 and Table 1. These parameters show a significantly stronger and much more linear relation than we found comparing model and ASAR derived spectra bin by bin. This supports that there is reliable wave information in the ASAR wave spectra that is suitable for assimilation.

Table 1: Comparison between ASAR Image Mode data (set 3) and collocated WAM model data with respect to significant wave height (HM0), peak period (Tp), and mean period (Tm02). The WAM spectra have been interpolated into the ASAR domain before comparison.

	ASAR mean	Interp. WAM mean	Mean dev.	Std. dev.	RMS	R^2
HM0(m)	2.0	4.5	2.5	0.9	2.6	0.7
Tp(s)	14.3	12.7	-1.7	1.4	2.2	0.9
Tm02(s)	13.2	8.7	-4.6	2.2	5.1	0.5

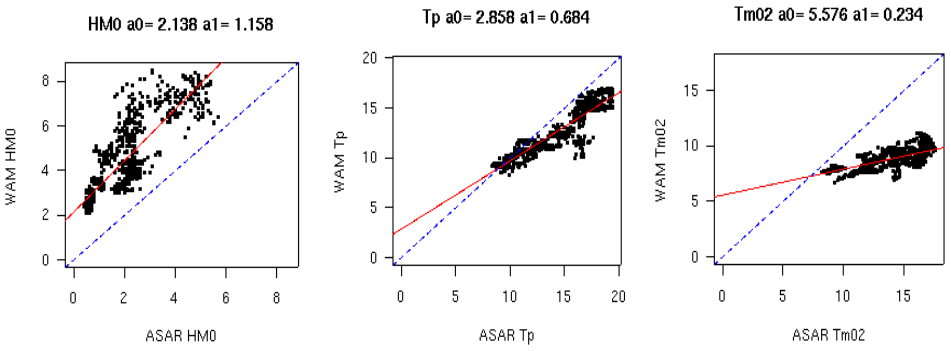

Figure 4: Scatter plot of significant wave height (HM0), peak period (Tp), and mean period (Tm02) for parameters derived from ASAR observations (horizontal axis, data set 3) vs. collocated WAM spectra that are interpolated to ASAR spectral domain.

Note that even though the collocated WAM spectra have been interpolated to the ASAR spectral domain in this comparison, they only formally cover the same frequency range. ASAR do not detect wave energy for its high frequencies, and is not recommended to be used for wave lengths longer than 250 m. This explains some of the bias seen in Figure 4, particularly for HM0.

4. Qualitative tests of R matrices

The statistical study shows a weak relation between bins of the ASAR derived wave spectra vs. the corresponding bins of the reference WAM model wave spectra. The results are therefore not sufficient to determine the diagonal **R** matrix properly and a set of qualitative tests has been performed as described in the following.

The ASAR spectra are more reliable for the lowest frequencies, than the higher ones, particularly with respect to directional information. For higher frequencies the data quality depends increasingly on the direction. The SAR instrument measures the waves in range direction most accurately. It is not recommended to trust SAR data for waves shorter than 250 m, i.e. frequency no. 9 and above [*Kerbaol et al.*, 1998; *Hasselmann and Hasselmann*, 1991].

We have chosen to let the **R** matrix vary with the wave frequency and be constant with respect to geographical direction. Six sets of values for R have been tested. The values R1, R I – V are given in

columns of Table 2. The columns show how R-values vary with the 24 ASAR frequencies. In order to avoid an unphysical discontinuity in the assimilated spectra, we let **R** smoothly change from giving significant weight to the ASAR spectrum for low frequencies (small values in **R**), to literally no weight for high frequencies (e.g. **R**-values of 200.0 in Table 2).

A case study testing 5 different sets of **R** matrix values (Table 2) has been performed. The chosen case is located in the middle of the North Atlantic (50N, 34 E) using an ASAR derived wave spectrum from 2004-10-20 23:48 UTC and model analysis time 12 min. later, at 24:00 UTC. The wind is moderate and the wind sea and swell are going in the same direction. The resulting wave spectra are shown in Figure 5 and 6 where the wave state is presented in polar plots, which represent the combination of waves in a single geographical location. The directions in the plot corresponds to geographical directions, where upward corresponds to waves going northward. The circles represent different wave frequencies, with 0 Hz in the center and an increase in frequency of 0.05 Hz/circle. The colors and contours represent different wave energy ranges (intensities). The red arrow shows peak direction, while the wind speed is represented by the characteristic wind symbol. Figure 5 upper panel shows the ASAR observation spectrum (left) and the WAM first guess (right).

R1 (Figure 5, middle left panel): ASAR and first-guess spectra are given about equal weight for all frequencies by **R** (although the low-pass filter downscales the ASAR weight for higher frequencies). The assimilated spectrum is a smooth combination of the observations and first-guess spectra.

R I and R II (Figure 5, middle right panel and lower left panel): We see in the assimilated spectra that the weight of the ASAR spectrum is more and more limited to the inner part, i.e. lowest frequencies. The wave spectra are less smooth for increasing frequencies, particularly for the R II parameter set.

R III and R IV (Figure 5 lower right panel and Figure 6 left panel): These two parameter sets are similar to the R I set, and differ only by the minimum non-zero value in **R**. The minimum value for set R III is 1.0, giving approx. equal weight to observation and first-guess spectrum for the lowest frequencies. The minimum value for set R IV is 1.5, giving more weight to the first-guess spectrum than the observation. We see that the geographically broad low-frequency part from ASAR becomes less distinct with R III and R IV, giving somewhat smoother and more realistically shaped spectra.

R II and R V (Figure 5 middle left panel and lower left panel): These parameter sets differ only by the minimum non-zero **R**-value of 0.5 and 1.5, respectively. They give a smooth cut-off at about 250 m wave length, avoiding weight from SAR for shorter waves than 250 m (Figure 5 lower left panel and Figure 6 right panel). This is in accordance with recommendations in the literature [*Kerbaol et al.*, 1998; *Hasselmann and Hasselmann*, 1991].

We conclude that for operational use it will be safe and reasonable to choose the R V set, which gives the majority (approx. 2/3) of the weight to the first-guess WAM spectrum. However, in a study where the intention is to investigate the potential impact of the assimilation, whether positive or negative, it is better to choose the R1 or R II set.

4.1 General quality of ASAR spectra

A report about intercomparisons of directional wave spectra from ASAR, buoys and the WAM model was published as part of the EnviWave project [*Fouqes et al.*, 2005]. They conclude from visual inspection that about 60% of the collocated ASAR spectra had no apparent correspondence to the WAM or the buoy spectra. They describe a number of reasons for this, and conclude that the current quality parameters distributed with the Wave Mode spectra are insufficient for proper screening.

Table 2: 1st col.: Frequency number (order) in ASAR wave spectrum. 2-6th col.: Observation covariance matrix parameter sets of diagonal values with respect to frequencies, R I-V. 7-10th col.: ASAR wave periods, wavelengths, wave numbers and frequencies.

Freq. {1,..,24}	R1	R I	R II	R III	R IV	R V	ASAR T (s)	ASAR L (m)	ASAR waven.(1/m)	ASAR freq.(Hz)
1	1,0	1,0	1,0	1,0	1,5	1,5	22,6	800,4	0,007850	0,044157
2	1,0	0,5	0,5	1,0	1,5	1,5	21,1	693,5	0,009060	0,047438
3	1,0	0,5	0,5	1,0	1,5	1,5	19,6	601,3	0,010450	0,050948
4	1,0	0,5	0,5	1,0	1,5	1,5	18,3	521,4	0,012050	0,054709
5	1,0	0,5	0,5	1,0	1,5	1,5	17,0	452,0	0,013900	0,058759
6	1,0	0,5	0,5	1,0	1,5	1,5	15,8	391,7	0,016040	0,063120
7	1,0	0,5	0,5	1,0	1,5	1,5	14,8	339,6	0,018500	0,067788
8	1,0	0,5	1,0	1,0	1,5	1,5	13,7	294,6	0,021330	0,072788
9	1,0	1,0	2,0	1,0	1,5	2,0	12,8	255,3	0,024610	0,078185
10	1,0	2,0	5,0	2,0	2,0	5,0	11,9	221,4	0,028380	0,083960
11	1,0	3,0	20,0	3,0	3,0	20,0	11,1	191,9	0,032740	0,090179
12	1,0	4,0	200,0	4,0	4,0	200,0	10,3	166,4	0,037760	0,096846
13	1,0	8,0	200,0	8,0	8,0	200,0	9,6	144,2	0,043560	0,104020
14	1,0	16,0	200,0	16,0	16,0	200,0	9,0	125,1	0,050240	0,111710
15	1,0	32,0	200,0	32,0	32,0	200,0	8,3	108,4	0,057950	0,119980
16	1,0	64,0	200,0	64,0	64,0	200,0	7,8	94,0	0,066850	0,128860
17	1,0	128,0	200,0	128,0	128,0	200,0	7,2	81,5	0,077100	0,138390
18	1,0	256,0	200,0	256,0	256,0	200,0	6,7	70,7	0,088930	0,148620
19	1,0	500,0	200,0	500,0	500,0	200,0	6,3	61,3	0,102580	0,159620
20	1,0	999,0	200,0	999,0	999,0	200,0	5,8	53,1	0,118320	0,171430
21	1,0	999,0	200,0	999,0	999,0	200,0	5,4	46,0	0,136480	0,184120
22	1,0	999,0	200,0	999,0	999,0	200,0	5,1	39,9	0,157420	0,197740
23	1,0	999,0	200,0	999,0	999,0	200,0	4,7	34,6	0,181580	0,212370
24	1,0	999,0	200,0	999,0	999,0	200,0	4,4	30,0	0,209440	0,228080

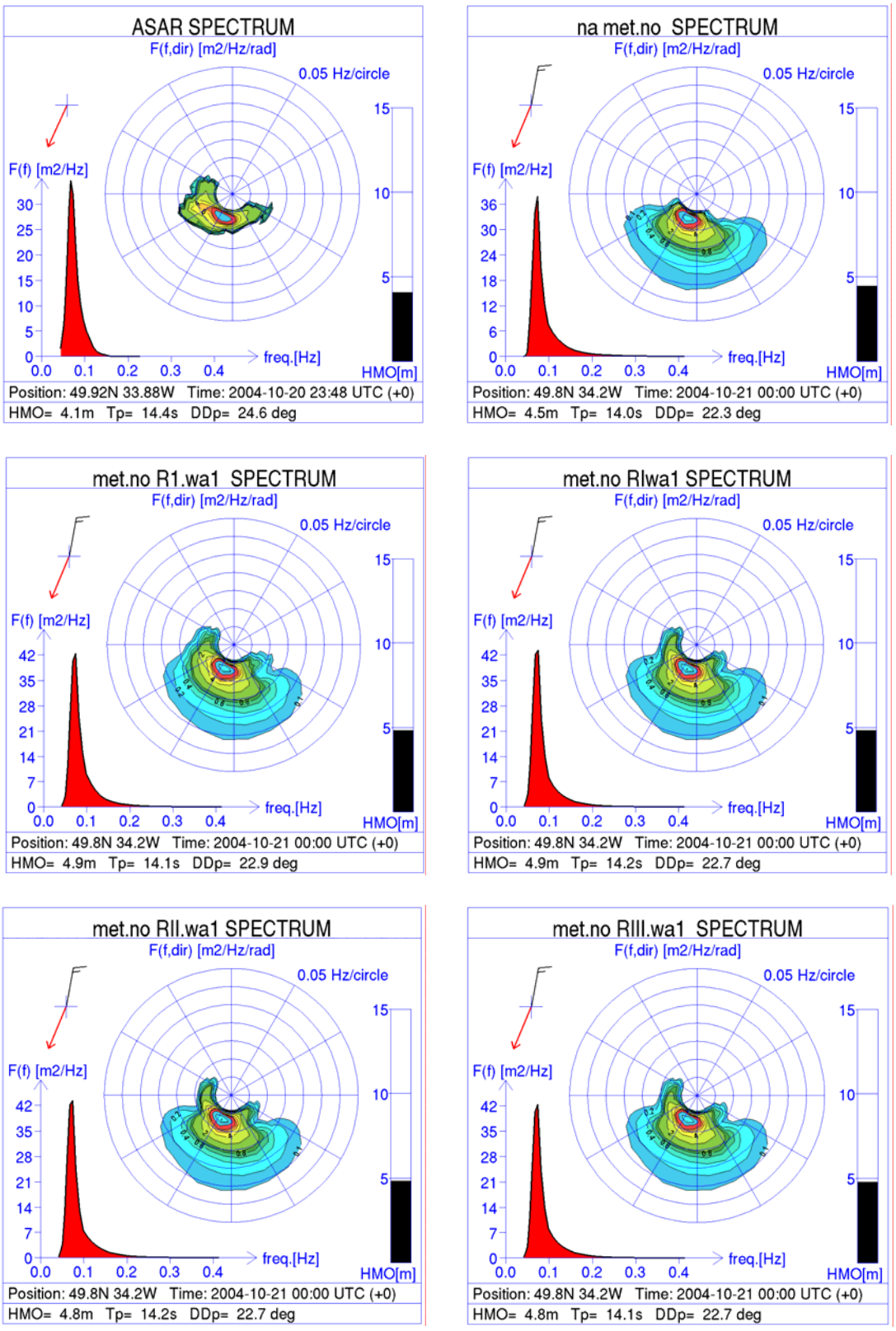

Figure 5: Assimilation of a single ASAR spectrum (top left) in WAM model. Non-assimilated spectrum (top right). The other spectra show the results using different sets of observation covariance matrices R1, R I, R II, R III, given in Table 2

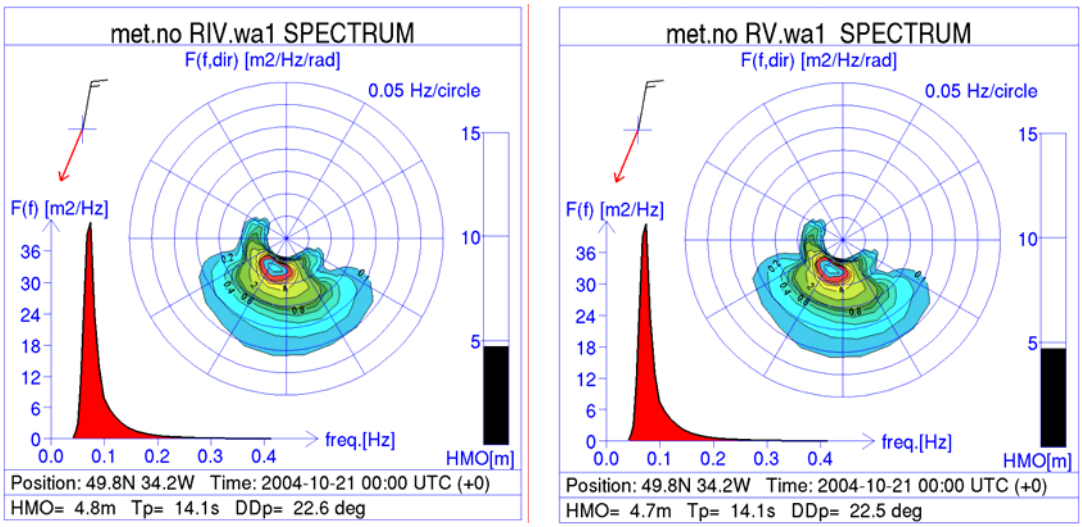

Figure 6: Results from assimilated WAM spectra from assimilation of single ASAR spectrum using observation covariance matrix RIV (left) and RV (right) given in Table 2. Compare these figures with ASAR spectrum (top left in Figure 5) and non-assimilated spectrum (top right in Figure 5).

5. Impact study in the North Atlantic

The impact study was originally planned for wave spectra derived from ASAR Wave Mode in the North Sea and Norwegian Sea, since Wave Mode is supposed to be the default mode of the ENVISAT ASAR over oceans. However, there is hardly any Wave Mode data in this region. This is exemplified by Figure 7, which shows all available wave spectra from ASAR Wave Mode for this region, for 3 weeks in February 2005. There are no data along the Norwegian Coast, and only a few spectra in the North Sea and Norwegian Sea. The reason for this is probably that ASAR in this region is operated in other modes than Wave Mode.

The impact study has in stead been run for the North Sea and the Norwegian Sea based on a set of ASAR wave spectra generated from ASAR Image Mode, from 7 days in January 2005 delivered by KSAT and NORUT. The map in Figure 1 illustrates the model area. The study includes about 900 wave spectra.

The wave spectra has been derived from Image Mode and carefully checked by NORUT, both by automatic and manual quality control. We therefore assume that this data set has at least the quality of Wave Mode derived wave spectra, and hence at least the quality that can be expected from operational use of ASAR derived wave spectra. The distance between neighboring wave spectra are about 20 km in azimuth direction and about 38 km in range direction.

The assimilation scheme is described in the previous section. In the present impact study the observation error covariance matrix “R I” is applied. The model grid has a resolution of 0.5 * 0.5 deg. and is shown in Figure 1. The same grid is used in the operational runs of WAM at met.no.

In the following we focus on results that coincide with Norwegian oil rigs due to independent measurements available in these locations. These oil rigs are marked with green squares in Figure 8 and 10. The blue anchors illustrate the model output locations in the grid point closest to either an ASAR spectrum or an oil rig. The wave states are presented in the same type of polar plots as described in the previous section.

The polar spectra in Figure 9 and 11 show the waves for several oil rigs, model spectra without assimilation (top row), with ASAR assimilation (2nd row), and the ASAR spectra (3rd row).

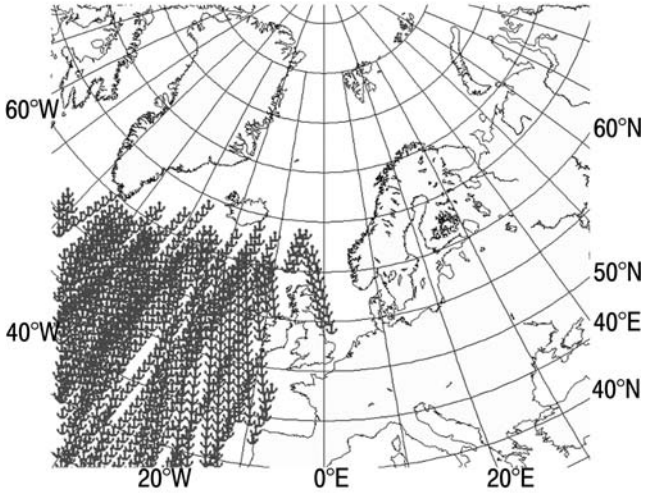

Figure 7: The anchors show ASAR Wave Mode data for 3 weeks (in February 2005) in the North Atlantic Ocean. There were no data along the Norwegian coast and only a few in the North Sea and Norwegian Sea.

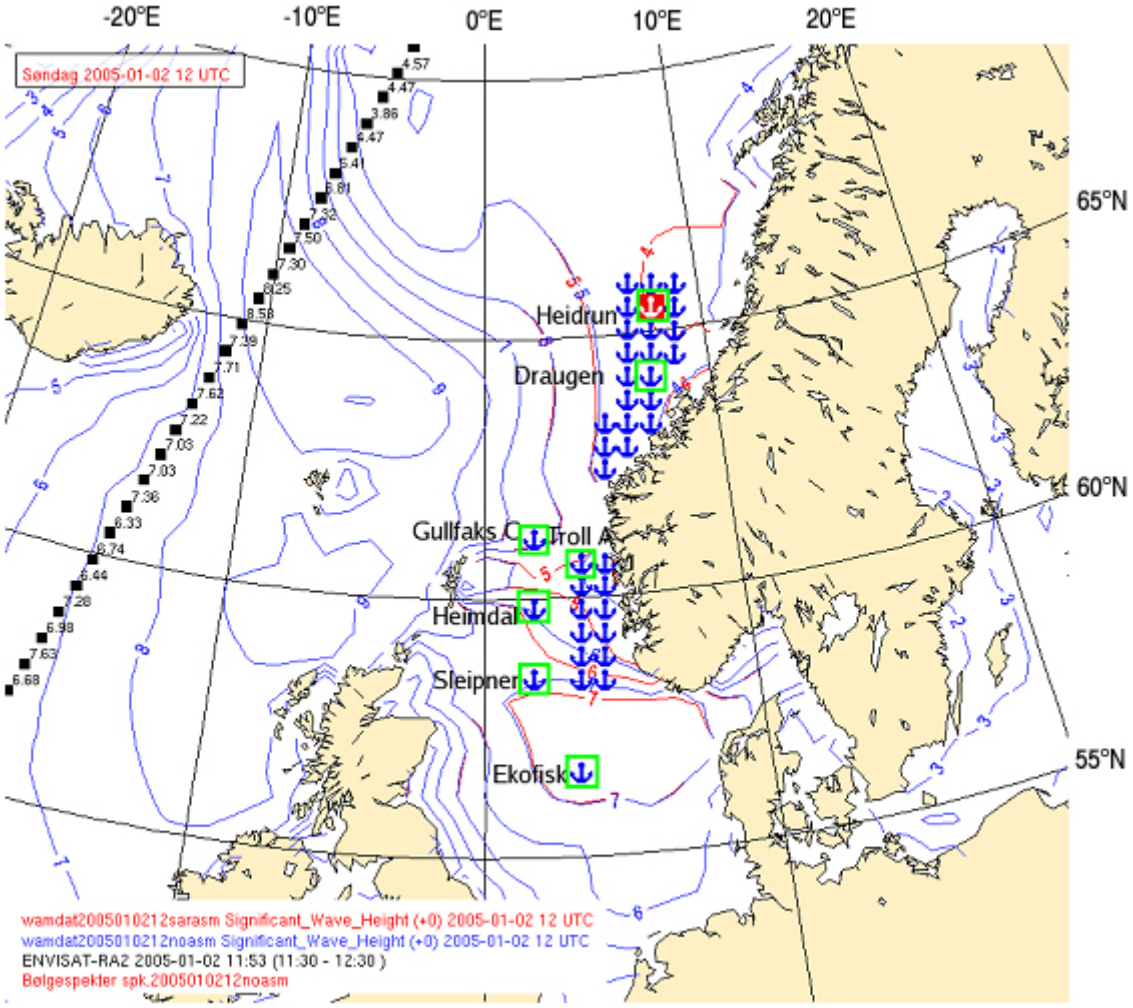

Figure 8: The blue anchors show the closest grid points to ASAR observations and oil rigs, where model spectra have been calculated for the date 2005-01-02 12 UTC. The significant wave height at analysis time is shown as contour plot, where blue shows the non-assimilated model state, and red shows the assimilated model state where it deviates from the non-assimilated state. The observations marked with black squares are significant wave heights from ENVISAT RA-2.

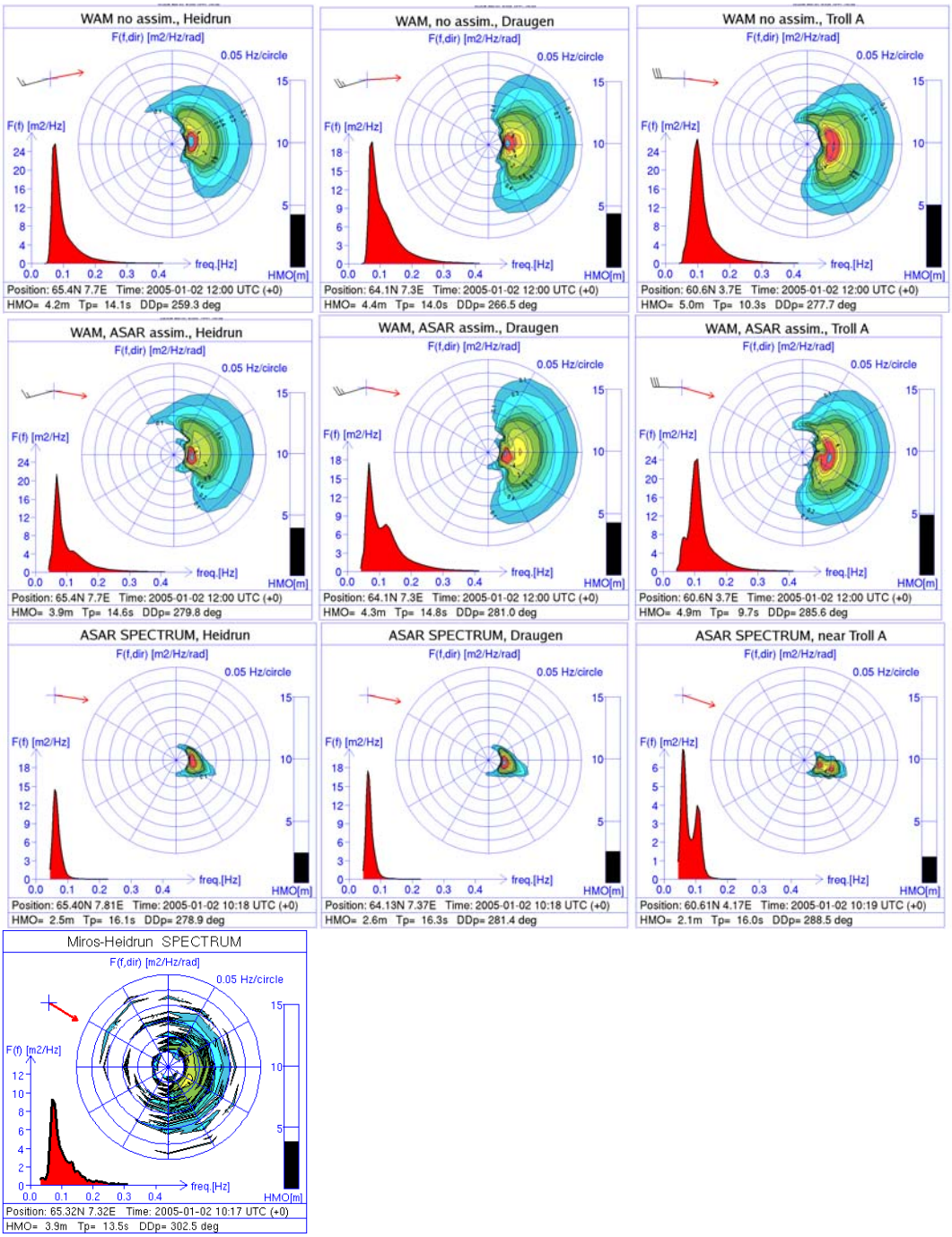

Figure 9: Polar plot of wave spectra for the oil rigs Heidrun, Draugen, and Troll A, on 2005-01-02. See Figure 8 for locations. **Top row**: WAM model spectra without assimilation. **2nd row**: WAM model spectra with ASAR assimilation. **3rd row**: ASAR spectra at or near the oil rig. **Bottom left**: Wave spectrum from local Miros radar at Heidrun.

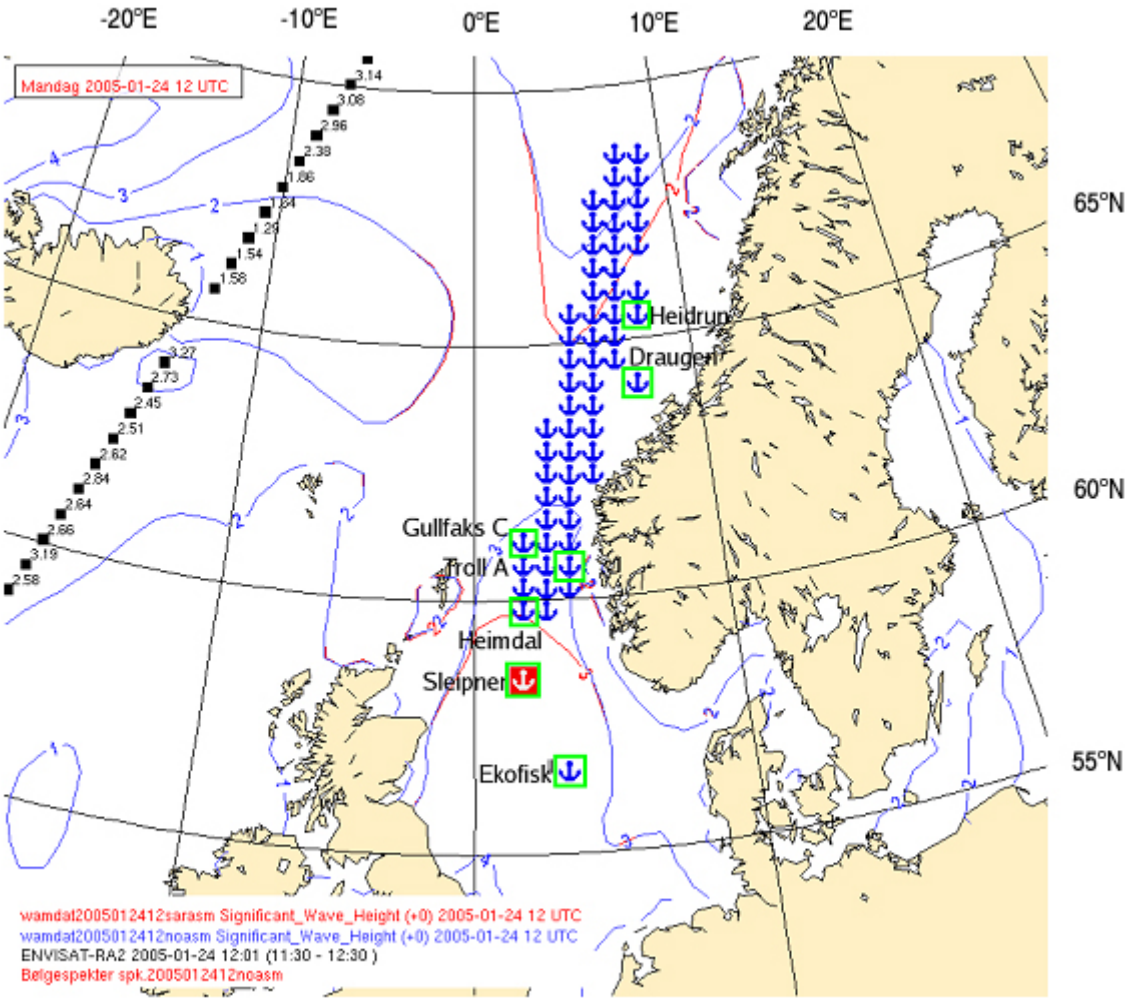

Figure 10: The blue anchors show the closest grid points to ASAR observations and oil rigs, where model spectra have been calculated for the date 2005-01-24 12 UTC. The significant wave height at analysis time is shown as contour plot, where blue shows the non-assimilated model state, and red shows the assimilated model state where it deviates from the non-assimilated state. The observations marked with black squares are significant wave heights from ENVISAT RA-2.

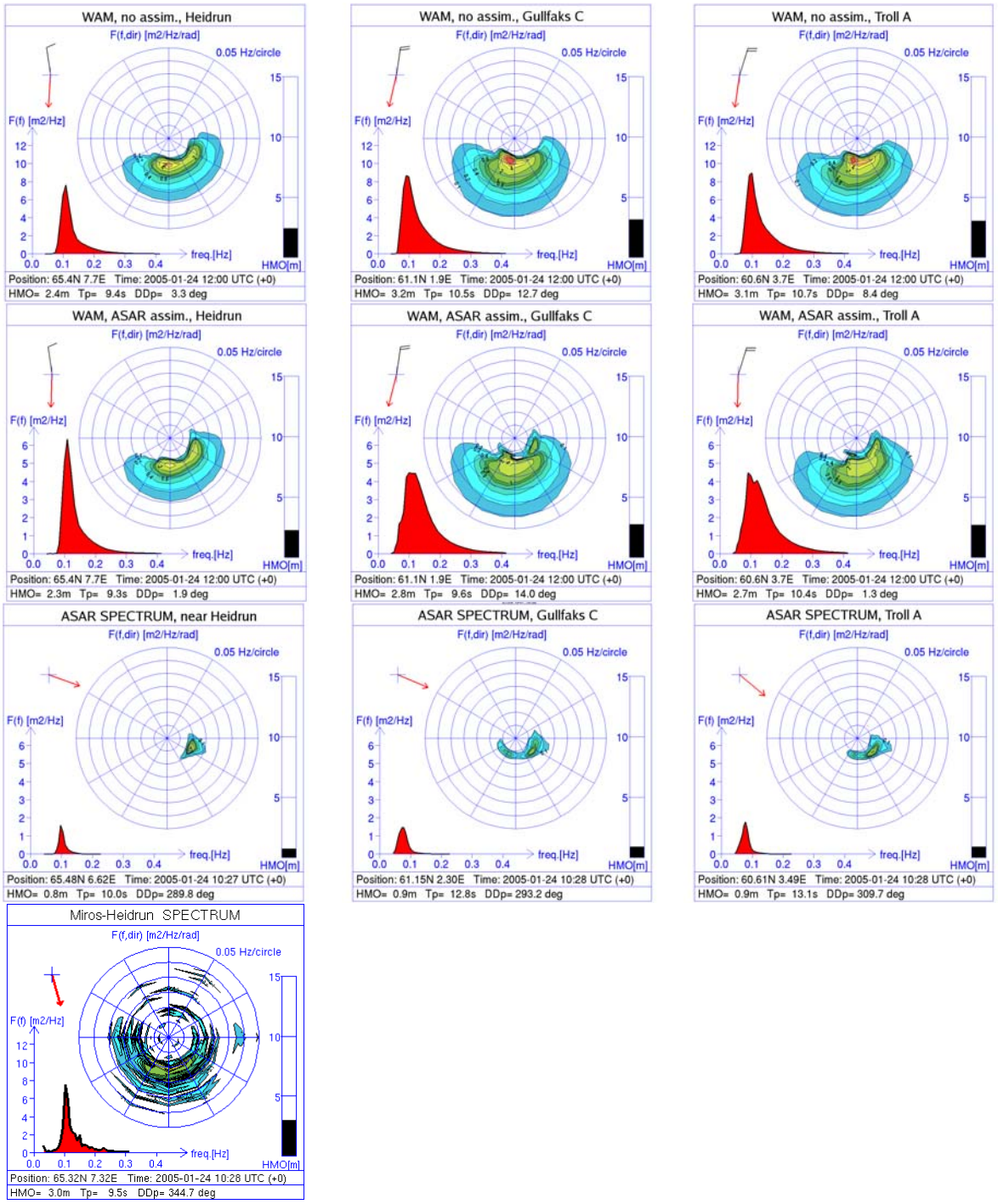

Figure 11: Polar plot of wave spectra for the oil rigs Heidrun, Gullfaks C, and Troll A, on 2005-01-24. See Figure 10 for locations. **Top row**: WAM model spectra without assimilation. **2nd row**: WAM model spectra with ASAR assimilation. **3rd row**: ASAR spectra at or near oil rig. **Bottom left**: Wave spectrum from local Miros radar at Heidrun.

Some oil rigs have directional wave spectra measured by local Miros radars. 3 examples of Miros wave spectra can be compared with the corresponding ASAR spectrum nearby, and model spectra with and without assimilation of the ASAR spectrum in Figure 9, 11 and 12. We see that Miros wave spectra are quite different from ASAR wave spectra, both with respect to frequency range and noise. Nevertheless, Miros spectra provides useful information for comparison with model and ASAR spectra.

The ASAR spectra and the non-assimilated WAM model agree reasonably well, and the assimilation gives just moderate adjustments. If we assume Miros spectra to be our best reference, the assimilation of ASAR at Heidrun in Figure 9 improves the spectrum, with respect to significant wave height, peak direction and

wave intensity profile (heave spectrum) although the small “wings of the swell “ seen for the lowest frequencies in the assimilated spectrum, seem unrealistically sharp. In Figure 11 the model (with and without assimilation) matches the Miros spectrum better than the ASAR spectrum. There is a small positive impact in peak direction but for the other parameters the impact is rather negative.

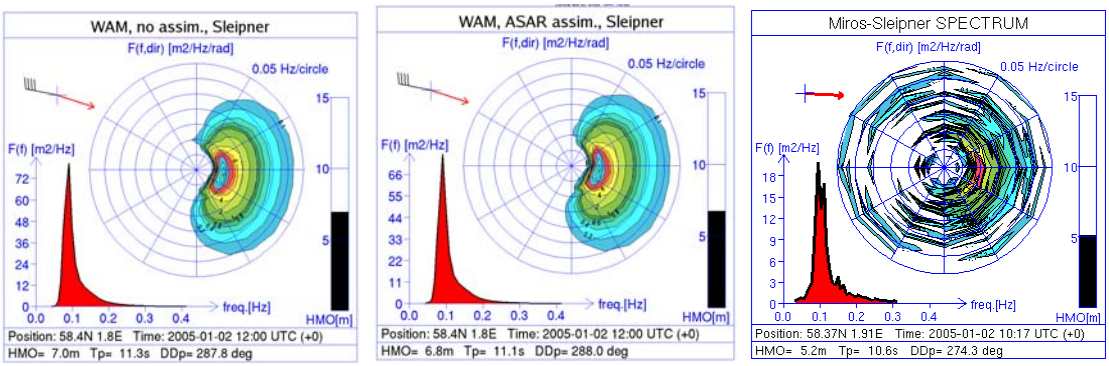

Figure 12: Wave spectra from model with and without ASAR assimilation and local Miros radar at Sleipner oil platform, 2005-01-02.

In Figure 12 we see model spectra for the oil rig Sleipner with and without assimilation compared with local Miros spectrum. There is no ASAR spectrum close to Sleipner (see Figure 8) and the assimilation impact is modest. However, the intensity in the heave spectrum (F(f) profile in Figure 12), peak period and significant wave height decrease toward the levels of the Miros spectrum upon assimilation, giving a positive impact.

5.1 Comparing model with local observations of significant wave height

Local measurements of significant wave height are available for several oil rigs, and these have been compared with our model estimates in order to study the assimilation impact. Figure 13 shows the difference in significant wave height (SWH) between the WAM model and local SWH observations (derived from Miros radar spectra) at oil rigs. For the pink line in Figure 13 the model includes ASAR assimilation, and for the blue line the model has been run without assimilation. Each line represents the difference between model and local measurement of significant wave height during a 36-hour prognosis time, starting at analysis time at the left. The ASAR assimilations do in all cases decrease the significant wave height. In some cases this reduces the error while in other cases it increases the error.

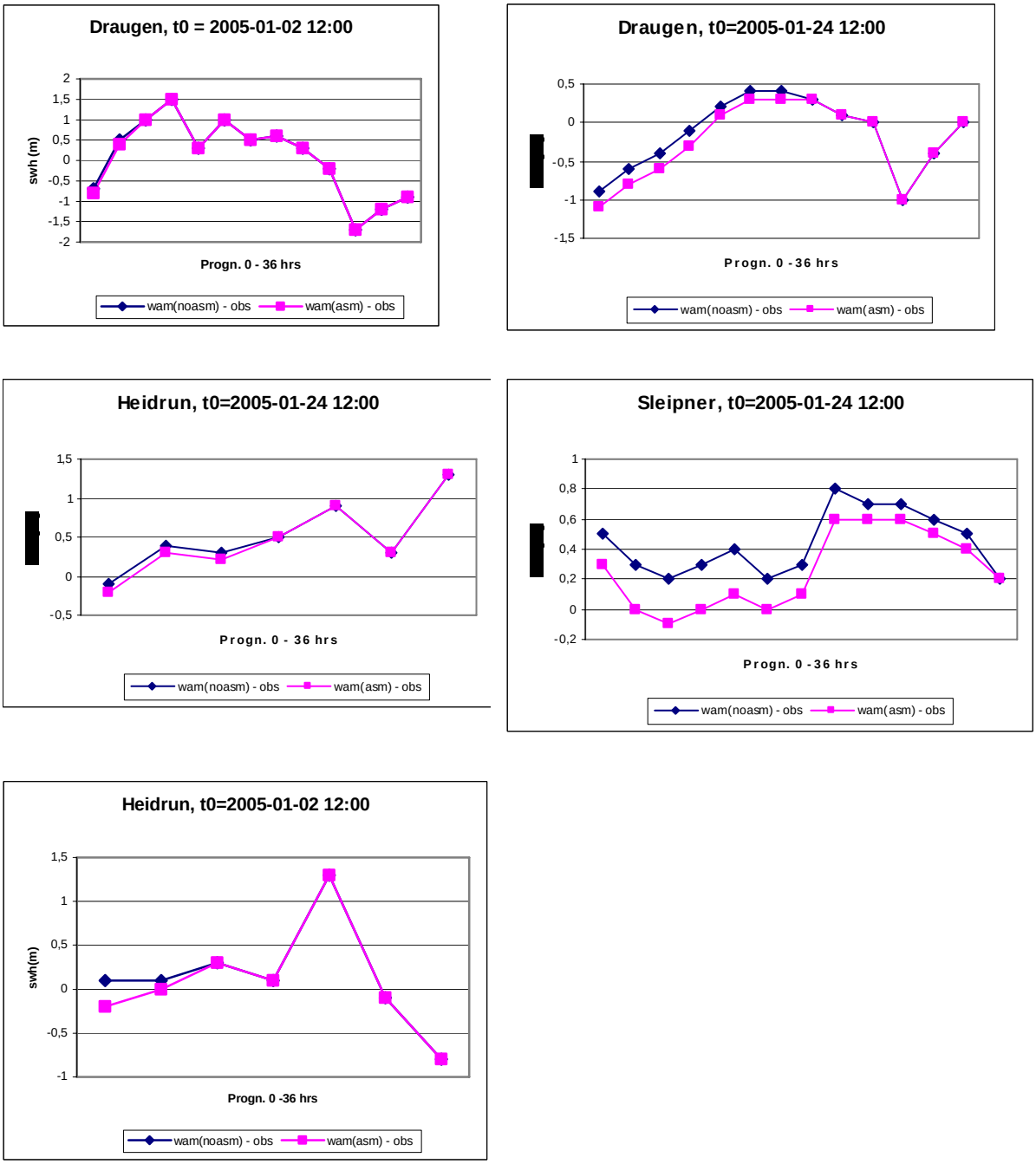

Figure 13: The model has been run with ASAR assimilation (pink squares) and without assimilation (blue diamonds) in 36-hour prognosis. The figures show the difference in significant wave height (swh) between the WAM model and local HM0 observations derived from Miros radar wave spectra at oil rigs. The model time development from analysis time (left point) is shown along the horizontal axis, every 6th hour for Heidrun, and every 3rd hour for Draugen and Sleipner.

6. Conclusions on ASAR wave data assimilation

The limited number of ASAR data and reference values available do not allow for a proper statistical study. It is therefore difficult to draw an absolute conclusion about the impact based on these experiments. However, some general conclusions can be made. The assimilation of ASAR spectra tends to decrease the significant wave height. The results show positive impact in some cases and negative impact in about the same number of cases, so there is no clear trend of neither positive nor negative impact.

The limited amount of Wave Mode data in our areas is clearly a problem. Wave spectra from Image Mode are an alternative when available. To give impact Image Mode data need to be regularly ordered, and

currently this will be too expensive for only the purpose of wave spectra assimilation. However, data collected for other purposes can also be utilized for wave information.

Objective data control remains a main problem for operational data assimilation of SAR data, due to poor correspondence between the ASAR derived wave spectra, buoy data and the WAM model [*Fouques et al.*, 2005]. An automatic data control would need to be so restrictive in not admitting erroneous observations that most data would be rejected.

7. Aspects of future ASAR wave data assimilation

A key question for future use of ASAR derived wave spectra is the data quality and of course the availability of ASAR data. For met.no the important areas to cover is the North Sea and the Norwegian Sea and in particular the Barents Sea where there is an increasing offshore activity. There are very few conventional observations in the Barents Sea, and the sea state in this region is dominated by weather systems originating from poorly observed areas in the Arctic. As documented in this study, the ENVISAT ASAR Wave Mode data do not give sufficient coverage in these areas. In fact in the largest parts of the Norwegian Sea and in the Barents Sea there are no data. An alternative data source is the Canadian Radarsat SAR mission. These data are in use for sea ice, oil spill and ship detection in the North Sea, Norwegian Sea and Barents Sea. As a following up of the EnviWave project met.no are investigating the possibility to derive ocean wave spectra routinely from these Radarsat data. If available close to real time these data can be useful for monitoring and nowcasting, and provided a proper data quality control the data can also be considered for assimilation in regional WAM model as described in this report.

Given a stable supply of ocean wave spectra observations from SAR including a proper data quality control, we believe that there is a potential for improvements in the assimilation method, e.g. in the description of the error covariance matrices. The error covariance matrices control how much weight the observation is given in the assimilation and how the information is spread in space and in the wave spectrum. Further study of how the error is correlated in the wave spectrum, might give improvements to the background error covariances, and hence improvements to the assimilation.

The quality of ASAR derived wave spectra generally decreases for increasing frequencies, and we only assimilate the lower frequency part of the ASAR wave spectrum. In the present assimilation scheme the observation error covariances are fixed to a set of predefined values, which are partly based on the recommended general cut-off frequency for ASAR derived wave spectra. Static error covariance matrices are in accordance with traditional and common assimilation schemes. However, the overall quality of ASAR data also vary and each ASAR data set provides an estimated recommended cut-off frequency that is specific for this data set. In order to exploit this dynamic information about the quality of the wave spectra, the observation error covariance matrix could be implemented such that it is dynamically updated and adjusted to the specific cut-off frequency that is optimal for each wave spectrum or each set of wave spectra.

The data quality also varies within the ASAR spectrum, because the ASAR instrument observes waves going parallel with the satellite slightly more accurately than perpendicular to the satellite track. This means that the error in each bin depends on the SAR antenna's look angle versus the wave propagation direction. Ideally this could be taken into account when deriving the statistics, (although it would require a larger data set than the current one). Further, this directional variation in reliability could be incorporated in the assimilation scheme by making the diagonal observation error covariance matrix (**R**) dynamic with respect to direction. Each element of **R** represents a geographical wave propagation direction. The elements of R for each direction could e.g. be scaled depending on the SAR antenna's look angle, which can be calculated from the direction between the current and the previous wave spectrum locations. This may improve the ASAR assimilation.

8. ASAR wave data in operational monitoring and nowcasting

The ENVISAT ASAR wave data are used in operational monitoring and nowcasting at met.no. The ASAR wave spectra can be displayed by using the meteorological workstation software DIANA [*Bergholt et al.*, 2005], which is developed and widely used at met.no (Figure 14). Using DIANA the forecaster combines data from various sources to get optimal information for his analysis of the weather and sea state. The data sources are numerical weather prediction models, ocean and wave prediction models, in situ observations and satellite data. The idea in using ASAR for wave nowcasting was therefore to enable displaying of wave spectra information together with wave model output and relevant meteorological information. An example on how this is done is given in Figure 14. This is indeed very useful for the operational wave forecasters, however it is as for data assimilation dependent on a regular supply of ASAR derives quality-controlled spectra.

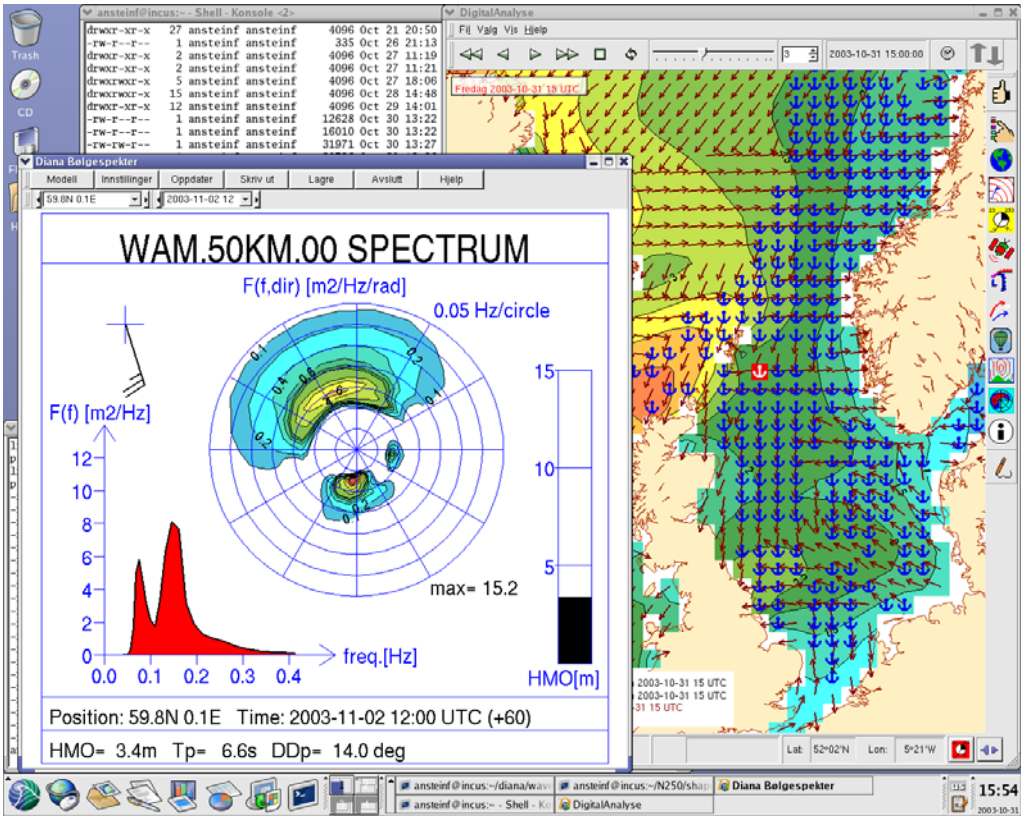

Figure 14: Example of screen dump of wave analysis system at met.no developed as part of the EnviWave project.

References

Aouf, L., J.-M. Lefèvre, D. Hauser (2006), Assimilation of Directional Wave Spectra in the Wave Model WAM: An Impact Study from Synthetic Observations in Preparation for the SWIMSAT Satellite Mission. *J. Atm. and Oceanic Technology*, *23*(3), 448-463.

Bergholt, L., A. Christoffersen, A. Foss, H. Korsmo, E. Martinsen, and J. Schulze (2005), Diana: A free Meteorological Workstation, paper presented at 10th Workshop on Meteorological Operational Systems, ECMWF, Reading, UK, 14-18 November. http://met.no/diana/

Bidlot, J.-R. (2002), SAR data assimilation, altimeter background check and a new WAM grid decomposition in CY25R3, *Memorandum R60.0/JG/0274*, ECMWF, Reading, UK.

Bouttier F. and P. Courtier (2002), Data assimilation concepts and methods, *Met. Training Course Lecture Notes, Data Assimilation*, ECMWF, Reading, UK.

Breivik, L.A., M. Reistad, H. Schyberg, J. Sunde, H.E. Krogstad, H. Johnsen (1998), Assimilation of ERS SAR wave spectra in an operational wave model, *J. Geophys. Res.*, *103*(C4), 7887-7900.

Engen, G., P.W. Vachon, H. Johnsen, F.W. Dobson (2000), Retrieval of ocean wave spectra and RAR MTF´s from dual-multi-polarization SAR data, *IEEE Transactions on Geoscience and Remote Sensing, 38*(1), 391-403, doi:10.1109/36.823935.

Fouques, S., H.E. Krogstad, I.M. Skaar (2005), Intercomparisons of directional wave spectra from ASAR, buoys and the WAM model: the co-location database, *SINTEF report STF90 A05084, ISBN 82-14-03801-4*, SINTEF IKT Applied Mathematics, Trondheim, Norway.

Hasselmann, K., and S. Hasselmann (1991), On the nonlinear mapping of an ocean wave spectrum into a synthetic aperture radar image spectrum, *J. Geophys. Res.*, *96*, 10713-10729.

Hasselmann, S., P. Lionello, and K. Hasselmann (1997), An optimal interpolation scheme for assimilation of spectral wave data, *J. Geophys. Res.-Oceans*, *102*(C7), 15823-15836.

Heiberg, H, A.M. Brattli (2005), Assimilation of ASAR ocean wave spectra in WAM – supplementary code comments, *met.no note 10*, Norwegian Meteorological Institute, Oslo, Norway.

Johnsen, H. (2005a), Development and Application of Validated Geophysical Ocean Wave Products from Envisat ASAR and RA-2 Instruments, *EnviWave Final Report*, Norut, Tromsø, Norway, 15 June.

Johnsen, H. (2005b), ENVISAT ASAR Wave Mode Product Description and Reconstruction Procedure, *Report 1, ENVISAT mission document, ISSN 1503-1705, ISBN 82-7747-126-2*, NORUT, Tromsø, Norway.

Kalnay, E (2003), *Atmospheric Modelling, Data assimilation and Predictability*, Cambridge University Press, Cambridge, UK.

Kerbaol, V., B. Chapron, and P. W. Vachon (1998), Analysis of ERS-1/2 synthetic aperture radar wave mode imagettes, *J. Geophys. Res.-Oceans*, *103*(C4), 7833-7846.

Voorrips, A. C., V. K. Makin, S. Hasselmann (1997), Assimilation of wave spectra from pitch-and-roll buoys in a North Sea wave model, *J. Geophys. Res.-Oceans*, *102*(C3), 5829-5849.

WAMDI Group (1988), The WAM model – A third generation wave prediction model, *J. Phys. Oceanogr.*, *18*(12), 1775-1810.

Aarnes, J. (2003), Iterative methods for data assimilation and an application of ocean state modelling, *Report No. STF42 A03015, ISBN 82-14-02909-0*, SINTEF Applied Mathematics, Oslo, Norway.